Research Article

Guan-yong Shi*, Ting-an Zhang*, Li-ping Niu, and Zhi-he Dou

Study on physical properties of Al_2O_3 -based slags used for the self-propagating high-temperature synthesis (SHS) – metallurgy method

https://doi.org/10.1515/htmp-2022-0046 received June 15, 2022; accepted June 20, 2022

Abstract: The Al₂O₃-based slags are playing important roles in the preparation of Cu-Cr alloy through self-propagating high-temperature synthesis (SHS) – Metallurgy method. However, the current research on Al₂O₃-based slag is mainly concentrated on steel metallurgical slag and electroslag remelting slag, and the research on aluminum thermal reduction slag with high content of Al₂O₃ is still insufficient. Therefore, systematic studies of the physical properties of slag with high aluminum content were carried out in the present work, and the influence of CaF₂, CaO, MgO, SiO₂, and Na₃AlF₆ on viscosities, liquidus temperatures, densities, and surface tensions of high Al₂O₃ content slags was measured and analyzed. The results indicated that CaO and CaF₂ have positive effects on the physical properties of Al₂O₃-based slags, MgO has positive effects when its content is not over 3%, and SiO₂ and Na₃AlF₆ have negative impacts. CaO, CaF₂, and MgO (not over 3%) could be used as additives to improve the metallurgical performance of Al₂O₃-based slags in aluminothermic reduction-slag refining method.

Keywords: Al₂O₃-based slag, SHS-metallurgy, viscosity, liquidus temperatures, density, surface tension

PACS number: 60

e-mail: zta2000@163.com

Li-ping Niu, Zhi-he Dou: Key Laboratory for Ecological Metallurgy of Multimetallic Ores (Ministry of Education), Northeastern University, Shenyang, 110004, China

1 Introduction

As an excellent medium-voltage vacuum circuit breaker contact material, Cu-Cr alloy is widely used in modern industry [1,2]. Dou et al. developed a new preparation method of Cu-Cr alloy by Self-propagation High-temperature Synthesis (SHS) – metallurgy process [3–5]. In this method, high-temperature melts produced by aluminothermic reduction were transferred to the induction furnace for carrying out the slag refining process. Thus, the composition of the refining slag is controlled by the composition of the aluminothermic reduction slag. In the aluminothermic reduction processes, Al₂O₃ is one of the major products and some additives are added to lower its melting point, so the slags used in this method are aluminate melts with high Al_2O_3 content. In both the aluminothermic reduction process and the slag refining process, the properties of slag have crucial impacts on the removal of inclusions and separation of alloy melts and slag; therefore, the physical properties of Al₂O₃-based slags are playing significant roles in this method.

Accurate physical property values for slag melts are necessary for optimizing and improving the productive processes [6–8]. Although many experimental measurements of molten slag's physical properties have been carried out, the available data are still scarce compared to the needs of today's technology, especially in the Al_2O_3 -based systems. Currently, the research on Al_2O_3 -based slags focuses on slags used in the steelmaking process and electroslag remelting process [9–12], and the research on high Al_2O_3 content slags which were used in the thermite reduction processes is not sufficient.

The aim of the present work is to investigate the physical properties of the aluminate melts used in the aluminum thermal reduction–slag refining process systematically. The effects of different additives such as CaF_2 , CaO, MgO, SiO_2 , and Na_3AIF_6 on the viscosities, liquidus temperatures,

^{*} Corresponding author: Guan-yong Shi, Institute of Green Metallurgy and Process Intensification, Jiangxi University of Science and Technology, Ganzhou 341000, China,

e-mail: shigy@qq.com

^{*} Corresponding author: Ting-an Zhang, Key Laboratory for Ecological Metallurgy of Multimetallic Ores (Ministry of Education), Northeastern University, Shenyang, 110004, China,

densities, and surface tensions were studied. The results of this study will provide a theoretical basis for the design of slag components in the aluminothermic reduction—slag refining process.

2 Experimental procedures

2.1 Experiment materials and equipment

All slags in the present work were synthesized with the analytical-grade reagents provided by Sinopharm Chemical Reagent Co. Ltd. All reagents were annealed in a muffle furnace to eliminate moisture and volatile impurities. CaF_2 and Na_3AlF_6 were annealed at 773 K (500°C) for 6 h; CaO, Al_2O_3 , CaO, and CaO, and CaO, were annealed at 1,273 K (1,000°C) for 4 h.

Considering that the preparation of Cu–Cr alloy by self-propagating metallurgy is carried out in graphite crucible, and the main components in the slag are relatively stable, the crucibles used in the experiment were made by graphite. The crucible is prepared from high-purity, high-density fine structure graphite (the density is not less than $1.85 \, \mathrm{g \cdot cm^{-3}}$, the carbon content is more than 99.95%, and the average particle diameter is $25 \, \mu \mathrm{m}$), and the inner wall is polished. Ultrasonic cleaning is used to remove graphite powder from the crucible, and the cleaned crucible is dried at $250 \, ^{\circ}\mathrm{C}$ for $24 \, \mathrm{h}$.

CaO can combine with Al_2O_3 to form a series of low melting point compounds, so on the basis of our previous studies and phase diagram of CaO-Al₂O₃ system, a slag with $w(CaO):w(Al_2O_3)=1:2$ was selected as the base slag, and different amounts of CaF₂, CaO, MgO, SiO₂ and

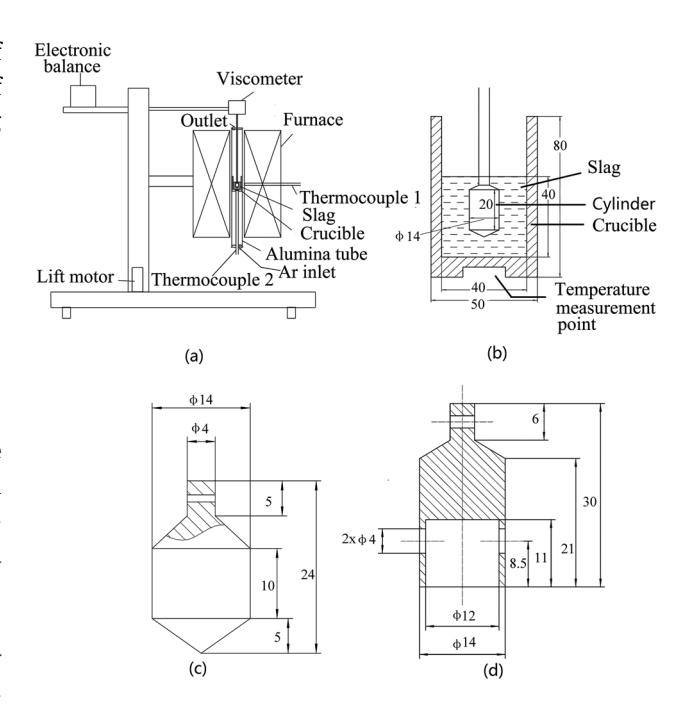


Figure 1: Schematic figure of experimental equipment: (a) type RTW-10 experimental apparatus for melts physical properties measurement; (b) crucible and cylinder used for the viscosity measurement; (c) molybdenum bob used for the density measurement; and (d) molybdenum ring used for the viscosity measurement.

 ${
m Na_3AlF_6}$ were added into the base slag to find out their influence on viscosities, liquidus temperatures, densities, and surface tensions. Table 1 gives the chemical compositions of all the samples used in the present work.

The physical properties measurements were carried out with an RTW-10 melts property analyzer. The schematic diagram of the experimental apparatus is shown in Figure 1. An electric resistance furnace with U-shape

Table 1: Composition of slag samples (mass %)

Samples	CaO	Al_2O_3	Additive	Samples	CaO	Al_2O_3	Additive
CA0	33.33	66.67	0	CAF7	20.00	40.00	40CaF ₂
CA1	32.50	65.00	2.5CaO	CAM1	32.50	65.00	2.5MgO
CA2	31.67	63.33	5CaO	CAM2	32.33	64.67	3MgO
CA3	30.83	61.67	7.5CaO	CAM3	32.00	64.00	4MgO
CA4	30.00	60.00	10CaO	CAM4	31.67	63.33	5MgO
CA5	26.67	53.33	20CaO	CAM5	31.33	62.67	6MgO
CA6	23.33	46.67	30CaO	CAM6	31.00	62.00	7MgO
CA7	20.00	40.00	40CaO	CAM7	30.67	61.33	8MgO
CAF1	32.50	65.00	$2.5CaF_2$	CAS1	33.00	66.00	1SiO ₂
CAF2	31.67	63.33	5CaF ₂	CAS2	32.67	65.33	2SiO ₂
CAF3	30.83	61.67	$7.5CaF_2$	CAS3	32.50	65.00	2.5SiO ₂
CAF4	30.00	60.00	10CaF ₂	CAS4	32.33	64.67	3SiO ₂
CAF5	26.67	53.33	20CaF ₂	CANAF1	32.50	65.00	2.5Na₃AlF ₆
CAF6	23.33	46.67	30CaF ₂	CANAF2	31.67	63.33	5Na ₃ AlF ₆

 $MoSi_2$ heating elements was used to melt the slags, the heating zone of the furnace is 250 mm long, and the constant temperature zone is 80 mm long. The temperature of the furnace was controlled within $\pm 1\,\mathrm{K}$ with a B-type (Pt-6wt% Rh/Pt-30wt% Rh) thermocouple. In order to improve the accuracy of slag temperature measurement, another B-type thermocouple was placed just under the crucible for the measurement of the temperature of melts (both positions of thermocouple and crucible were in the uniform temperature zone of the furnace).

2.2 Experiment methods

The internal rotating cylinder method (hanging wire method) was adopted for the viscosity measurements, and a stainless steel wire with a diameter of 0.19 mm is used to measure the torque experienced by the cylinder. Before the viscosity measurements, the viscometer was calibrated by castor oil of a known viscosity at room temperature. A molybdenum cylinder was adopted in the present study, and the rotating speed of the cylinder was 12 rpm.

The liquidus temperatures of the slags were estimated by the viscosity–temperature curve of the slag using Seetharaman's method. Seetharaman's research shows that the second derivative of viscous activation energy versus temperature shows obvious discontinuity near the liquidus temperature, and it is in accordance with the results determined using differential thermal analysis method. This method has been proven to be suitable for use in pure water, binary alloy, silicate, and aluminate melts [13–15].

The densities of the slags were measured by the Archimedes method. A molybdenum bob (as shown in Figure 1) was used to measure the density of the melt. The volume of the bob was determined by the pure water of a known density at room temperature, and the density of the melt was measured by the buoyancy of the bob in the melt.

The surface tensions of the slags were measured by the maximum tension method. The ring was made from molybdenum, and its dimension is given in Figure 1. The ring was dropped down to the surface of the molten slag, then was lifted up, and the maximum tension the ring receives was measured. For the sake of simplicity, the constant of the known diameter ring is calibrated by pure water, and then, the surface tension of the melt can be determined by the following formula:

$$\sigma = C \times D \times F_{\text{max}}, \tag{1}$$

where σ is the surface tension of the slag, N·m⁻¹; C is the instrument constant; D is the diameter of the barrel; and F_{max} is the maximum tension the ring receives.

The powders (~150 g) were weighed to the desired compositions and mixed for 1h to obtain homogeneous mixtures. The mixed slag was melted at 1,923 K (1,650°C) in a graphite crucible (diameter, 40 mm; depth, 70 mm) under the Ar atmosphere. The depth of the slag was adjusted to 40 mm with a steel rod with a diameter of 10 mm. The slag adhering to the steel rod is ground and used for X-ray diffraction (XRD) analysis. The furnace was kept at 1,923 K (1,650°C) for 1 h to ensure the melt was uniform. Then, the viscosity, density, and surface tension of the slag at 1,923 K (1,650°C) were measured. After that, the temperature decreased at a rate of 3 K (3°C)/min, and the viscosity was measured continuously until the viscosity started to rise rapidly. Finally, the liquidus temperatures of the slags were estimated by the viscosity-temperature curve. After the last measurement, the furnace was reheated to 1,923 K (1,650°C), and the spindle was lifted out of the slag.

3 Results and discussion

3.1 Effect of additives on the viscosity

The viscosity–temperature curves of all samples measured during the cooling process are presented in Figure 2, and the effects of CaF₂, CaO, MgO, SiO₂, and Na₃AlF₆ on viscosities at 1,650°C are shown in Figure 3.

As shown in Figure 2, the viscosities of all slags decreased with increasing temperature, as expected. Most of the viscosity-temperature curves presented "short-slag" features, and obvious inflection points can be found on the viscosity-temperature curves [16]. At higher temperature above the inflection point, since the slag temperature is still considerably higher than the temperature of the liquid, the viscosity increases slowly as the temperatures decreases. When the melt temperature is lowered to below the inflection point, the viscosity will begin to rise sharply, which is caused by the crystallization and solidification of the melts. Due to the slower rotation speed (12 rpm), the viscometer outputs data every 5 s, and the rate of increase in viscosity is so severe that the slag is completely solidified between the two outputs of the viscometer. Therefore, there is a big difference in the maximum viscosity value on the different viscosity curves. This is a significant difference between aluminate slag and silicate slag.

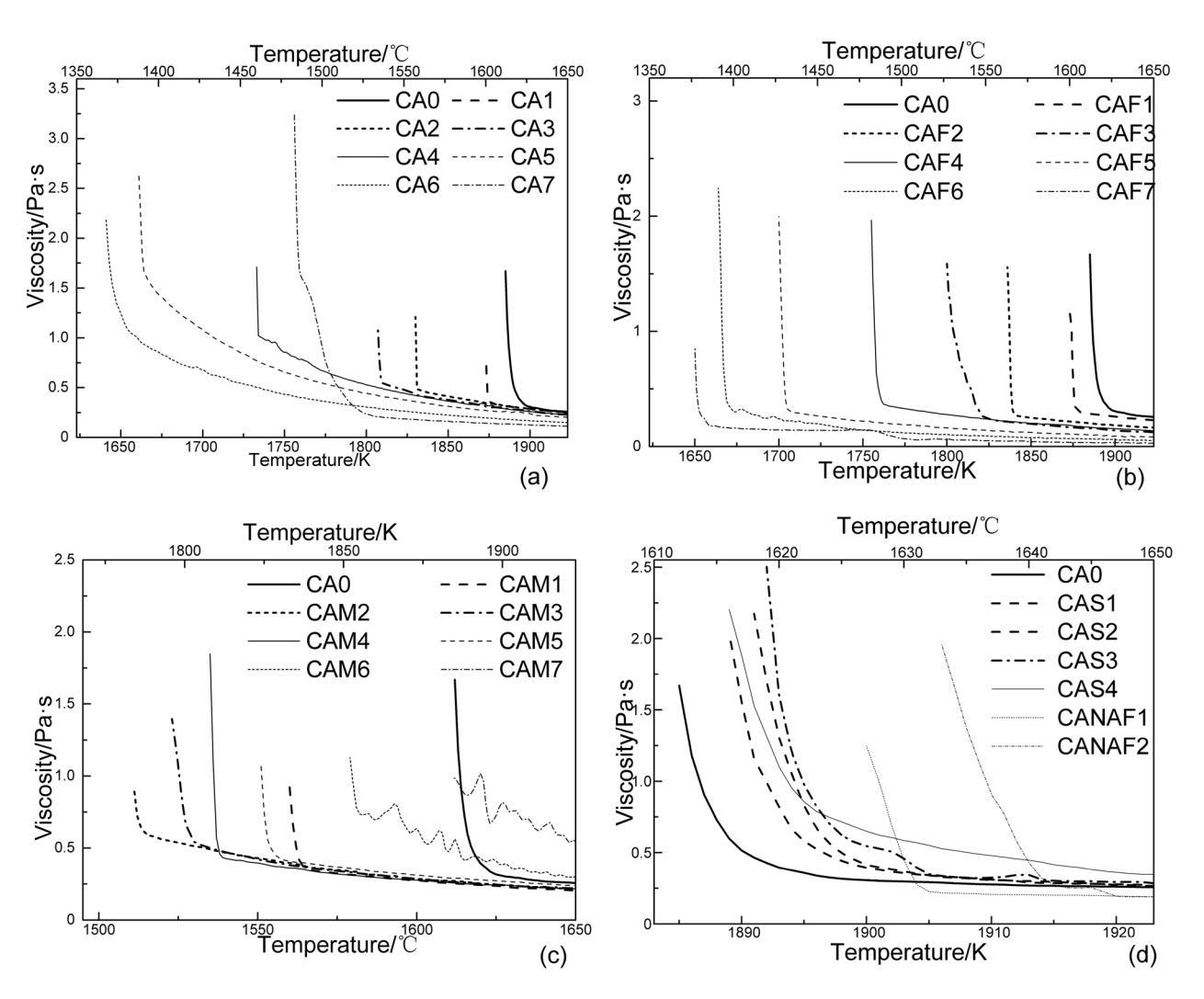


Figure 2: Effect of different additives on viscosity-temperature curves of slags: (a) CaO; (b) CaF2; (c) MgO; SiO2; and (d) Na3AlF6.

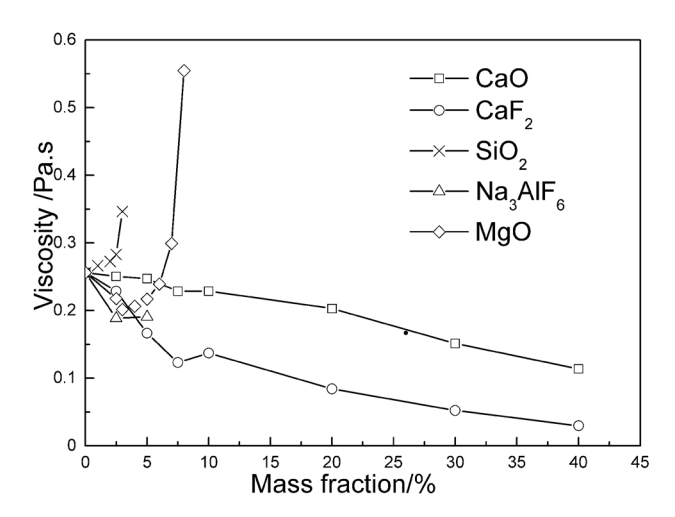


Figure 3: Effect of different additives on the viscosity of slags at 1,923 K (1,650°C).

The effect of CaO on the viscosity is shown in Figures 2a and 3. All melts have good fluidity, and with the increase in the amount of CaO up to 40%, the viscosity at 1,650°C decreased from 0.256 to 0.114 Pa·s. All curves have obvious inflection points, and the temperatures of the inflection points decreased with the amount of additive CaO increased to 30%. This can be explained on the basis of the fact that the change in CaO content could cause changes in melt structure. As a typical amphoteric oxide, in the aluminate slag melts, Al₂O₃ usually forms a network through Al-O-Al bonds, just like silica in a silicate melt. In recent years, there has been considerable research on the structure of alumina and aluminate melts [17–22]. The structural unit of the aluminate anion is very complicated, and it is generally believed that the coordination number of aluminum is 4, 5, and 6, namely, AlO₄,

 AlO_5 , and AlO_6 units. In some studies, there is also the presence of aluminum with a coordination number of 3. Although there are certain differences between different studies, it could be assumed that the Al ion in the aluminate melt is mainly in the form of a tetra coordinated AlO_4 tetrahedron. Due to the increases in the content of CaO, the dissociation of CaO would increase the availability of free oxygen ions (O^{2-}) in the melt, which results in the increases in the relative fraction of AlO_4 units and decreases in that of AlO_5 and AlO_6 units, thereby causing a decrease in the average coordination number of Al. Hence, with the increase in calcium oxide content in the melt, the relative amount of complex network structure within the slag decreases as non-bridged oxygen increases, and the viscosity of the slag decreases as the aluminate structure depolymerizes.

The effect of CaF₂ on the viscosity is shown in Figures 2b and 3. As shown in the figures, both the viscosities and the temperatures of the inflection points of the melts decrease with the increase in calcium fluoride content. The ability of CaF₂ to reduce the viscosity of slag is much higher than that of CaO. With the increase in the amount of CaF₂ up to 40%, the viscosity at 1,650°C decreased from 0.256 to $0.030\,Pa\cdot s$. When CaF_2 is added to the melt, the dissociation of CaF2 would increase the availability of fluoride ions (F⁻) in the melt and results in the formation of $[AlO_nF_{4-n}]^-$ complexes and the de-polymerization of the aluminate network, which resulted in a significant decrease in slag viscosities [23,24]. Each fluorite can provide two fluoride ions to the melt, and monovalent fluoride ions cannot form a network through Al-F-Al bond like oxygen ions. Therefore, CaF2 is more destructive to the melt network and has a stronger ability to lower the viscosity. When the mass fraction of CaF₂ is 40%, the viscosity of the slag has abnormally experienced an unusually dramatic increase between 1,500-1,480°C, and when the temperature continues to decrease, the viscosity curve shows significant fluctuations. This may be due to the liquid phase separation of the melt resulting in the conversion of the melt from Newtonian fluid to non-Newtonian fluid, as shown in the phase diagram.

The effect of MgO on the viscosity is shown in Figures 2c and 3. As shown in the figures, the viscosity–temperature curves of CAM1–CAM5 have obvious inflection points and present "short-slag" features. In the case of CAM6 and CAM7, when the mass fraction of MgO is 7–8%, the inflection points are not obvious and the viscosities of melts occur drastic fluctuations. With the increase in MgO content in the slag, the viscosities appeared to have a declining trend after an initial ascent, and the minimal point is 3%. Similar to CaO, when MgO is added to the melt, the dissociation of MgO would increase the

availability of free oxygen ions (O^{2-}) in the melt, resulting in a decrease in the relative amounts of the complex network structures, and the viscosity decreases with the depolymerization of the aluminate structures. However, when the MgO content is too high, since MgO can be combined with Al_2O_3 to form magnesium aluminum spinel, the melting point of the slag is increased, the superheat degree is lowered, and the viscosity is increased. When the MgO content continues to increase, it will lead to the formation of spinel particles in the melts and change the melts from Newtonian to non-Newtonian, causing instability of the viscosity–temperature curves.

Figures 2d and 3 show that as the content of SiO_2 in the melt increases, the viscosity of the melt gradually increases. When the SiO_2 content reaches 4%, the viscosity of the melt is too high and exceeds the upper limit of the range of the equipment. At the same time, the inflection points on the viscosity–temperature curves of the slag become inconspicuous, and the viscosity–temperature curves present "long-slag" features. On the one hand, the increase in the SiO_2 content reduces the CaO content and further reduces the free oxygen ions in the melt, and on the other hand, SiO_2 can form a network structure. These two factors work together, resulting in the improvement of the melt polymerization degree, and lead to the increase in the viscosity of slag.

As shown in Figures 2d and 3, with the increase in cryolite content, the viscosity of the slag decreases, but the temperature at the turning point continues to rise. When the cryolite content is increased to 7.5%, the viscosity of the melt is too high and exceeds the upper limit of the range of the equipment. This situation was unexpected, so the three groups of slag were repeatedly measured and achieved the same result. During the experiment, the slag containing cryolite violently volatilized and caused serious damage to the corundum furnace tube, so no further experiments were carried out. Like CaF₂, cryolite can provide fluoride ions into the melt, resulting in depolymerization of the complex structure of the melt, thereby reducing the viscosity of the melt.

3.2 Effect of additives on the liquidus temperature

The effects of CaF₂, CaO, MgO, SiO₂, and Na₃AlF₆ on liquidus temperatures are shown in Figure 4, and the XRD analysis results of the slag are shown in the figure.

The increase in CaO content in the slag results in the liquidus temperatures appearing to have an initial ascent

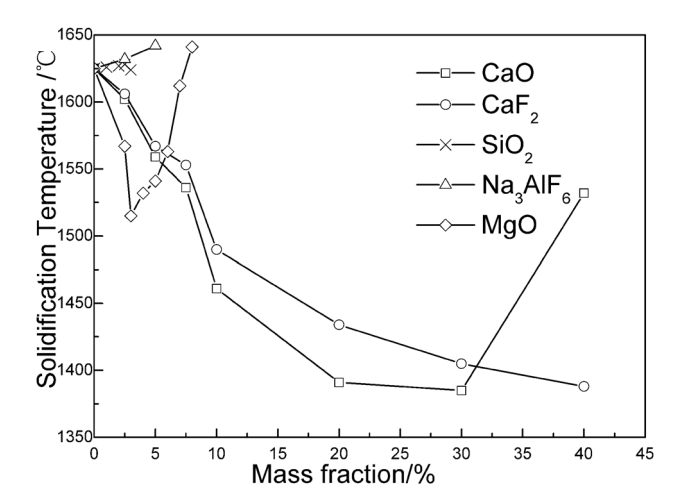


Figure 4: Effect of different additives on liquidus temperature of slags.

after a declining trend, and the minimal point is 30%. It can be seen from the phase diagram that there are a series of calcium aluminate compounds xCaO·vAl₂O₃ in the CaO-Al₂O₃ binary system. Among them, there are three congruent melting compounds (12CaO-7Al₂O₃, $C_{12}A_7$, 1,413°C; $CaO \cdot Al_2O_3$, CA, 1,602°C; and $CaO \cdot 2Al_2O_3$, CA₂, 1,762°C) and two incongruent melting compounds (3CaO·Al₂O₃, C₃A, 1,539°C; and CaO·6Al₂O₃, CA₆, 1,830°C). Therefore, as the CaO content in the slag increases, the phase of the system changes from a higher melting point of CA₂ and CA to a lower melting point of C₁₂A₇. When the addition amount of CaO is 30%, the composition of the slag is close to the eutectic point of $C_{12}A_7$ and C_3A . As a result, the liquidus temperature of the system appears minimum point when adding CaO into Al₂O₃-based slag. This result was confirmed by the XRD analysis of the slag (Figure 5).

The liquidus temperature decreased as the amount of CaF_2 increased. As shown in the phase diagram, CaF_2 has a lower melting point and can form low melting point compounds $3CaO\cdot 3Al_2O_3\cdot CaF_2$. XRD analysis showed that $3CaO\cdot 3Al_2O_3\cdot CaF_2$ did not appear in the slag, which may be due to the non-equilibrium solidification caused by the faster cooling rate. However, the diffraction intensity of CA_2 with a higher melting point in the slag is gradually reduced. Therefore, CaF_2 has the ability to reduce the liquidus temperature of the slag.

The increase in MgO content in the slag results in a decrease after an increase in liquidus temperature, and the minimal point is 3%. It is known from the binary phase diagram and XRD analysis that MgO has two effects on liquidus temperature. MgO and Al_2O_3 can form magnesium aluminate spinel with a high melting point, which

increases the liquidus temperature of the melts. At the same time, due to the combination of Al_2O_3 and MgO, the calcium aluminate phase in the melt will gradually change from CA_2 to CA and $C_{12}A_7$, which decreases the liquidus temperature of the melt. Therefore, a small amount of MgO can lower the liquidus temperature of the melt, and when the MgO content is too high, the liquidus temperature will rise due to the formation of spinel.

The liquidus temperature increased as the amount of SiO_2 increased, and the addition of SiO_2 causes the decrease in CaO content in slag. XRD analysis shows that as the SiO_2 content in the slag increases, the diffraction intensity of the CA phase gradually decreases, and the diffraction intensity of the CA2 phase gradually increased. This is because SiO_2 and CaO combine to form a glass phase, which reduces CaO combined with alumina. Therefore, SiO_2 can increase the content of the high melting point phase in the slag, thereby increasing its liquidus temperature.

The effect of Na_3AlF_6 on the liquidus temperature of the system is unexpected. Although its melting point is very low, and it could supply F^- ion into slag, the liquidus temperature increased as the amount of Na_3AlF_6 increased. On the basis of XRD analysis and our previous studies on the physical properties of $Na_2O-CaO-Al_2O_3$ [25], the increase in the liquidus temperature may be due to the formation of $3CaO\cdot Al_2O_3$ when the Na^+ cation is added to the slag.

3.3 Effect of additives on the density

The effects of CaF₂, CaO, MgO, SiO₂, and Na₃AlF₆ on densities are shown in Figure 6. The densities decreased as the amount of CaF₂ or CaO increased, and they increased as the amount of SiO₂ or Na₃AlF₆ increased. The increase in MgO content in the slag results in the densities appeared to have an initial ascent after a declining trend, and the minimal point is 3%. The density of melts is dependent on both the structure of the slag and the density of the component oxides. However, Alumina has a higher density, so the addition of other oxides having a lower density can reduce the density of the melt. At the same time, CaF₂, CaO, and MgO can also promote the depolymerization of the melt structure. Therefore, CaF2, CaO, and lower content of MgO reduce the density of calcium aluminate melt. The reason why SiO₂, Na₃AlF₆, and the higher content of MgO lead to an increase in melt density can be attributed to the increase in melt solidification temperature and the decrease in superheat of melt.

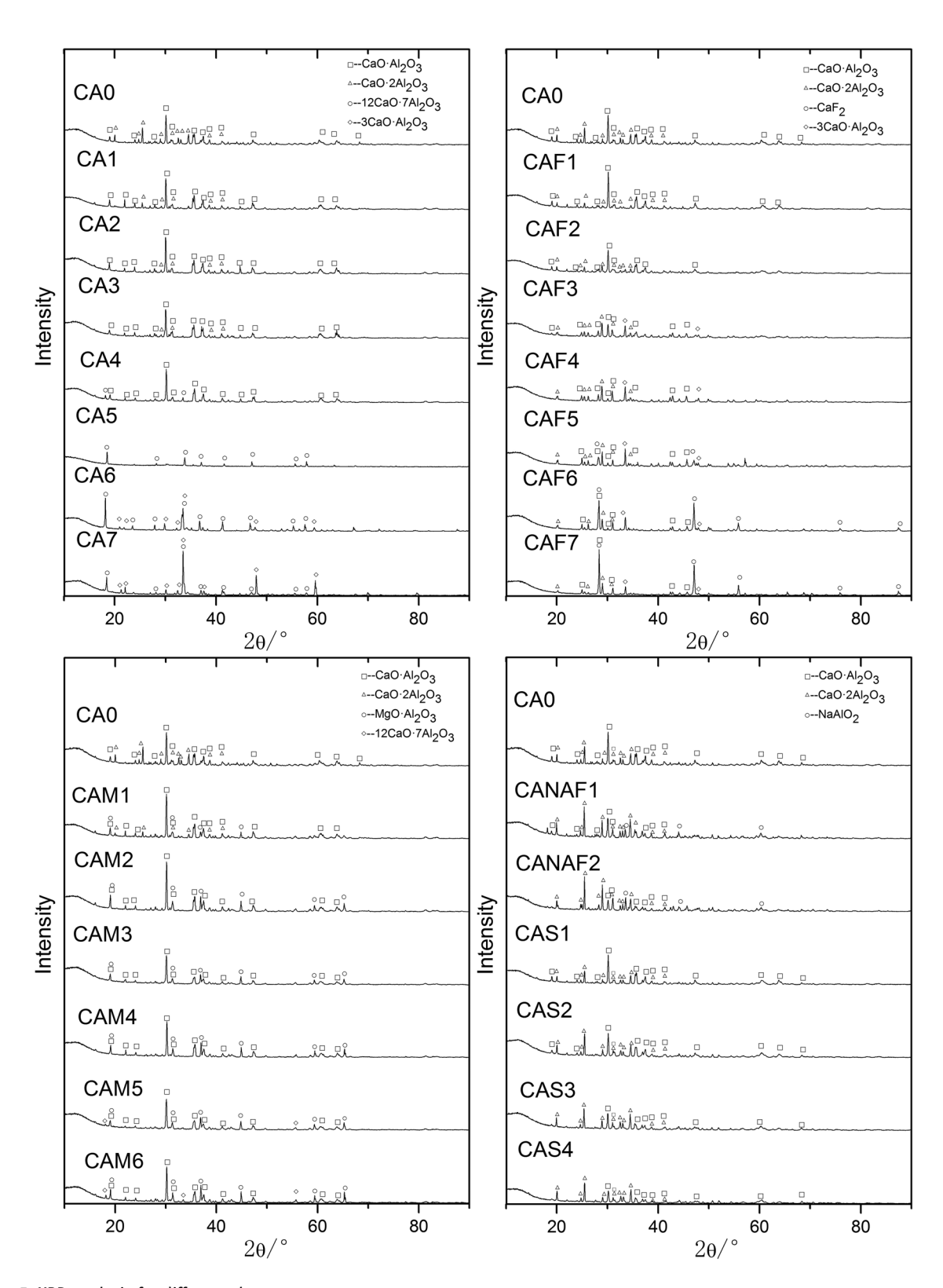


Figure 5: XRD analysis for different slags.

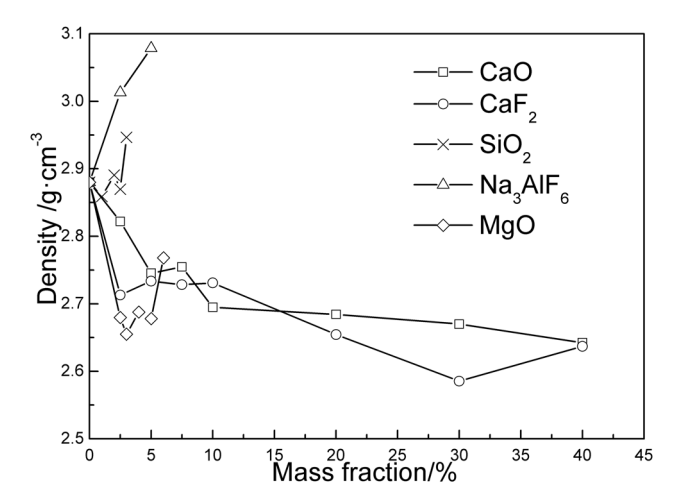


Figure 6: Effect of different additives on the density of slags at 1,923 K (1,650°C).

3.4 Effect of additives on the surface tension

The effects of CaF₂, CaO, MgO, SiO₂, and Na₃AlF₆ on surface tensions are shown in Figure 7.

With the increase in CaO or MgO content in the slag, the surface tensions appeared to have an initial ascent after a declining trend, and the minimal points are 10 and 3%, respectively. This phenomenon means that there may be structural changes in the melts, and further research is needed. The surface tensions of pure components CaO, MgO, and Al_2O_3 are 611, 547, and 684 mN·m⁻¹ at 1,650°C, respectively [26]. Since the surface tension of CaO and MgO is much lower than that of Al_2O_3 , the increase in CaO and MgO content in the melt tends to reduce its surface tension, and MgO with lower surface tension and smaller molecular weight is more capable of

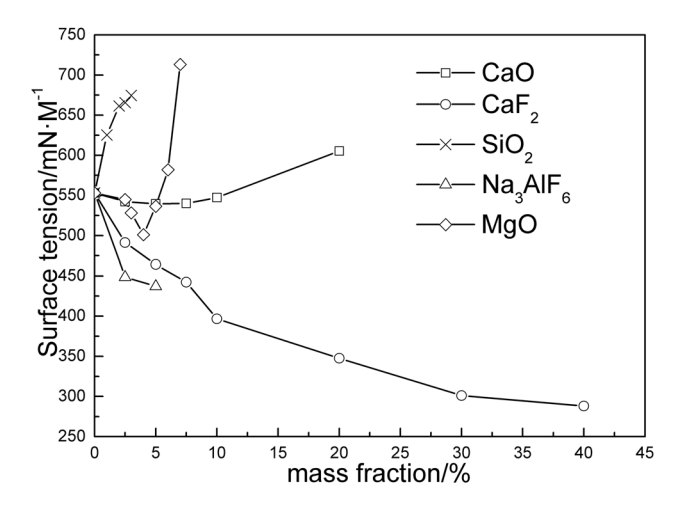


Figure 7: Effect of different additives on the surface tension of slags at $1,923 \text{ K} (1,650^{\circ}\text{C})$.

lowering surface tension. However, CaO and MgO have a small atomic weight, and an increase in their content increases the total number of ions in the melt; furthermore, MgO and CaO can provide free oxygen ions to the melt, causing the aluminate network to depolymerize. The lower degree of polymerization and the higher total number of ions in the melts could enhance the attraction forces between ions and thus increase the surface tension of the melts [27,28]. Due to these factors, as the content of CaO and MgO increases, the surface tension of the melt appeared to have an initial ascent after a declining trend.

The surface tensions decreased as the amount of CaF₂ or Na₃AlF₆ increased. The radius of fluoride and oxygen ions is very close, so their properties are similar. Therefore, fluoride ions can replace the position of oxygen ions in the aluminate melt. The number of charges of fluoride ions is smaller than that of oxygen ions, so its electrostatic potential is smaller than that of oxygen ions, and the interaction between ions is also smaller. Therefore, fluoride ions are concentrated on the surface of the melt, which significantly reduces the surface energy of the melts [29,30]. CaF₂ and Na₃AlF₆ can provide fluoride ions to the melt, so they are surfactants in the aluminate melt. At the same time, the surface tension of pure substances CaF₂ (220 mN·m⁻¹ at 1,650°C) [26] and Na_3AlF_6 (134 mN·m⁻¹ at the melting point, decreases with increasing temperature) [31] are much smaller than that of alumina. Due to these factors, both CaF₂ and Na₃AlF₆ can greatly reduce the surface tension of the slag.

Usually, SiO_2 in the slag is a surface-active substance. But in the present work, the surface tensions increased as the amount of SiO_2 increased. This may be caused by the fact that SiO_2 increases the liquidus temperature of the melt and lowers the degree of superheat.

4 Conclusions

The effects of different additives on the physical properties of high Al_2O_3 content slag which were used in the preparation of Cu–Cr alloy through aluminothermic reduction–slag refining process were studied in the present work. The results show as follows:

(1) When *w*(CaO):*w*(Al₂O₃) is 1:2 in the base slag, the increase of CaO content in the slag results in the decrease of viscosities and densities, and the liquidus temperatures and surface tensions appeared to have an initial ascent after a declining trend; the extreme points are at 30 and 10%, respectively. The increase in MgO content in the slag results in the viscosities,

densities, liquidus temperatures, and surface tensions appeared to have an initial ascent after a declining trend, the extreme points are at 3%. The increase in CaF_2 content in the slag results in a decrease in viscosities, densities, liquidus temperatures, and surface tensions. The increase in SiO_2 content in the slag results in the increase in viscosities, densities, liquidus temperatures, and surface tensions. The increase in Na_3AlF_6 content in the slag results in a decrease in viscosities and surface tensions, and the increase in densities and liquidus temperatures.

(2) It can be concluded that CaO and CaF₂ have positive effects on the physical properties of Al₂O₃-based slags, and they can be used as the additives in the SHS-metallurgy method. When the content is low, MgO has positive effects on the physical properties of Al₂O₃-based slag but it has a negative impact when the content is too high; therefore, it can be used as an additive but the content must be carefully controlled below 3%. SiO₂ and Na₃AlF₆ have negative impacts on the physical properties of Al₂O₃-based slags.

Acknowledgments: The authors gratefully acknowledge the fundamental support from The Open Fund Project of the Key Laboratory for Ecological Metallurgy of Multimetallic Ores (Ministry of Education), grant number NEMM2018004; The Science and Technology Research Project of the Education Department of Jiangxi Province, grant number GJJ180463; the Doctoral Scientific Research Foundation of JXUST, grant number jxxjbs17006; the National Natural Science Foundation of China, grant number 51674074, u1702253.

Funding information: The Open Fund Project of the Key Laboratory for Ecological Metallurgy of Multimetallic Ores (Ministry of Education), grant number NEMM2018004; The Science and Technology Research Project of the Education Department of Jiangxi Province, grant number GJJ180463; the Doctoral Scientific Research Foundation of JXUST, grant number jxxjbs17006; the National Natural Science Foundation of China, grant number 51674074, u1702253.

Author contributions: Guan-yong Shi: performed the experiment, data analyses and wrote the manuscript, Ting-an Zhang: methodology and reviewing the document, Li-ping Niu: contributed significantly to analysis and manuscript preparation, Zhi-he Dou: contributed significantly to analysis and manuscript preparation.

Conflict of interest: The authors state no conflict of interest.

Data availability statement: All authors can confirm that all data used in this article can be published in High Temperature Materials and Processes.

References

- [1] Si, S. H., H. Zhang, Y. Z. He, M. X. Li, and S. Guo. Liquid phase separation and the aging effect on mechanical and electrical properties of laser rapidly solidified Cu_{100-x}Cr_x alloys. *Metals*, Vol. 5, 2015, pp. 2119–2127.
- [2] Zhang, Z., J. Guo, G. Dehm, and R. Pippan. In-situ tracking the structural and chemical evolution of nanostructured CuCr alloys. *Acta Materialia*, Vol. 138, 2017, pp. 42–51.
- [3] Dou, Z. H., T. A. Zhang, H. A. Yu, L. P. Niu, X. L. Jiang and H. Yang. Preparation of CuCr alloys by thermit-reduction electromagnetic stirring. *International Journal of Minerals, Metallurgy and Materials*, Vol. 14, 2007, pp. 538-542.
- [4] Dou, Z. H., T. A. Zhang, Z. Q. Zhang, L. P. Niu, G. Z. Lv, Y. Liu, et al. Research on inclusions in CuCr alloy prepared by thermit reduction. 3rd International Symposium on High-Temperature Metallurgical Processing, *TMS 2012 Annual Meeting and Exhibition*, March 11–15, 2012, Orlando, 2012, pp. 265–270.
- [5] Dou, Z. H., C. Wang, G. Y. Shi, T. A. Zhang, and H. Y. Zhang. Study on inclusions in CuCr₂₅ prepared by thermit reductionelectromagnetic casting. 6th International Symposium on High-Temperature Metallurgical Processing, TMS 2015 Annual Meeting and Exhibition, March 15–19, 2015, Orlando, 2015, pp. 35–42.
- [6] Mills, K. C., L. Yuan, and R. T. Jones. Estimating the physical properties of slags. *Journal of Sourth African Minerals amd Metallurgy*, Vol. 111, 2011, pp. 649-658.
- [7] Mills, K. C., L. Yuan, Z. Li and G. H. Zhang. Estimating viscosities, electrical & thermal conductivities of slags. *High Temperature-High Press*, Vol. 42, 2013, pp. 237–256.
- [8] Seetharaman, S., L. Teng, M. Hayashi, and L. Wang. Understanding the properties of slags. ISIJ International, Vol. 53, 2013, pp. 1–8.
- [9] Mills, K. C. Chapter 9 in Slag atlas, 2nd Edition edited by Verein Deutscher Eisenhüttenleute (VDEh) Eds., Verlag Stahleisen, Dusseldorf, 1995, pp. 349-402.
- [10] Birol, B., G. Polat, and M. N. Saridede. Estimation model for electrical conductivity of molten CaF2-Al₂O₃-CaO slags based on optical basicity. *JOM*, Vol. 67, 2015, pp. 427-435.
- [11] Xu, J. F., J. Y. Zhang, C. Jie, F. Ruan and K. C. Chou. Experimental measurements and modelling of viscosity in CaO-Al₂O₃-MgO slag system. *Ironmak Steelmak*, Vol. 38, 2013, pp. 329–337.
- [12] Zhou, L. J., H. Li, W. L. Wang, D. Xiao, L. Zhang and J. Yu. Effect of Li₂O on the Behavior of melting, crystallization, and structure for CaO-Al₂O₃-based mold fluxes. *Metallurgical and Materials Transactions B: Process Metallurgy and Materials Processing Science*, Vol. 49, 2018, pp. 2232–2240.
- [13] Seftharaman, S., D. Sichen, S. Sridhar, and K. C. Mills.
 Estimation of liquidus temperatures for multicomponent silicates from activation energies for viscous flow. *Metallurgical and Materials Transactions B: Process Metallurgy and Materials Processing Science*, Vol. 31, 2000, pp. 111–119.

[14] Wang, Z., Q. F. Shu, and K. Chou. Estimation of liquidus temperature for B₂O₃- and TiO₂- containing fluoride free mould fluxes from activation energy for viscous flow and DTA measurements. CAN METALL QUART, Vol. 52, 2013, pp. 405-412.

DE GRUYTER

- [15] Xu, J. F., L. Tang, M. Q. Sheng, J. C. Li, J. Y. Zhang and K. Wan. Determination of liquidus temperatures from viscosity for CaO-Al₂O₃ based slags. 4th International Symposium on High-Temperature Metallurgical Processing, TMS 2013 Annual Meeting and Exhibition, 62, March 3-7, 2013, San Antonio, 2013, pp. 859-866.
- [16] Chu, S. J., H. H. Liu, S. S. Diao and T. Xu. Discrimination between long slag and short slag. Journal of University of Science and Technology Beijing, Vol. 2, 1995, pp. 19-23.
- [17] Ansell, S., S. Krishnan, J. K. R. Weber, J. J. Felten, P. C. Nordine, M. A. Beno, et al. Structure of liquid aluminum oxide. Physical Review Letters, Vol. 78, 1997, pp. 464-466.
- [18] Skinner, L. B., A. C. Barnes, P. S. Salmon, L. Hennet, H. E. Fischer, C. J. Benmore, et al. Joint diffraction and modeling approach to the structure of liquid alumina. Physical Review B, Vol. 87, 2013, id. 024201.
- [19] Akola, J., S. Kohara, K. Ohara, A. Fujiwara, Y. Watanabe, A. Masuno, et al. Network topology for the formation of solvated electrons in binary CaO-Al₂O₃ composition glasses. Proceedings of the National Academy of Sciences USA, Vol. 110, 2013, pp. 10129-10134.
- [20] Drewitt, J. W., L. Hennet, A. Zeidler, S. Jahn, P. S. Salmon, D. R. Neuville, et al. Structural transformations on vitrification in the fragile glass-forming system CaAl2O4. Physical Review Letters, Vol. 109, 2012, id. 235501.
- [21] Jahn, S. Amorphous materials. Properties, structure, and durability: Atomic structure and transport properties of MgO-Al₂O₃ melts: A molecular dynamics simulation study. AM MINERAL, Vol. 93, 2008, pp. 1486-1492.
- [22] Drewitt, J. W., S. Jahn, V. Cristiglio, A. Bytchkov, M. Leydier, S. Brassamin, et al. The structure of liquid calcium aluminates

- as investigated using neutron and high energy x-ray diffraction in combination with molecular dynamics simulation methods. Journal of Physics: Condensed Matter, Vol. 23, 2011, id. 155101.
- [23] Hyun, P. J., D. J. Min, and H. S. Song. Structural investigation of CaO-Al₂O₃ and CaO-Al₂O₃-CaF₂ slags via fourier transform infrared spectra. ISIJ International, Vol. 42, 2002, pp. 38-43.
- [24] Kim, T. S. and J. H. Park. Structure-Viscosity relationship of low-silica calcium aluminosilicate melts. ISIJ International, Vol. 54, 2014, pp. 2031-40.
- [25] Shi, G. Y., T. A. Zhang, L. P. Niu, and Z.H. Dou. Influence of Na₂O on properties of CaO-Al₂O₃ slag. Journal of Northeastern University-Natural Science, Vol. 33, 2012, pp. 1000-1003.
- [26] Hanao, M., T. Tanaka, M. Kawamoto, and K. Takatani. Evaluation of surface tension of molten slag in multi-component systems. ISIJ International, Vol. 47, 2007, pp. 935-939.
- [27] Xu, J., J. Zhang, D. Chen, M. Sheng, and W. Weng. Effects of MgO content and CaO/Al₂O₃ ratio on surface tension of calcium aluminate refining slag. Journal of Central South University, Vol. 23, 2016, pp. 3079-3084.
- [28] Sukenaga, S., T. Higo, H. Shibata, N. Saito, and K. Nakashima. Effect of CaO/SiO₂ ratio on surface tension of CaO-SiO₂-Al₂O₃-MgO melts. ISIJ International, Vol. 55, 2015, pp. 1299-1304.
- [29] Suzuki, M., S. Tanaka, M. Hanao, and T. Tanaka. Evaluating composition dependence in surface tension of Si-Ca-Na-O-F reciprocal oxide-fluoride melts. ISIJ International, Vol. 56, 2016, pp. 63-70.
- [30] Dong, Y. W., Z. H. Jiang, Y. L. Cao, H. K. Zhang, and H. J. Shen. Effect of MgO and SiO2 on surface tension of fluoride containing slag. Journal of Central South University, Vol. 21, 2014, pp. 4104-4108.
- [31] Fernandez, R., T. Østvold, L. Pettersson, L. O. Öhman, J. Ruiz, E. Colacio, et al. Surface tension and density of molten fluorides and fluoride mixtures containing cryolite. Acta Chemica Scandinavica, Vol. 43, 1989, pp. 151-159.